

Children's Mercy Kansas City

SHARE @ Children's Mercy

Manuscripts, Articles, Book Chapters and Other Papers

4-2019

Splice-altering variant in COL11A1 as a cause of nonsyndromic hearing loss DFNA37.

Kevin T. Booth

James W. Askew

Zohreh Talebizadeh
Children's Mercy Hospital

Patrick L M Huygen

James Eudy

See next page for additional authors

Let us know how access to this publication benefits you

Follow this and additional works at: <https://scholarlyexchange.childrensmercy.org/papers>



Part of the [Medical Genetics Commons](#)

Recommended Citation

Booth KT, Askew JW, Talebizadeh Z, et al. Splice-altering variant in COL11A1 as a cause of nonsyndromic hearing loss DFNA37. *Genet Med.* 2019;21(4):948-954. doi:10.1038/s41436-018-0285-0

This Article is brought to you for free and open access by SHARE @ Children's Mercy. It has been accepted for inclusion in Manuscripts, Articles, Book Chapters and Other Papers by an authorized administrator of SHARE @ Children's Mercy. For more information, please contact hlsteel@cmh.edu.

Creator(s)

Kevin T. Booth, James W. Askew, Zohreh Talebizadeh, Patrick L M Huygen, James Eudy, Judith Kenyon, Denise Hoover, Michael S. Hildebrand, Katherine R. Smith, Melanie Bahlo, William J. Kimberling, Richard J H Smith, Hela Azaiez, and Shelley D. Smith

Splice-altering variant in *COL11A1* as a cause of nonsyndromic hearing loss DFNA37

Kevin T. Booth, BA^{1,2}, James W. Askew, MA³, Zohreh Talebizadeh, PhD⁴, Patrick L. M. Huygen, PhD⁵, James Eudy, PhD⁶, Judith Kenyon, BS¹, Denise Hoover, BS³, Michael S. Hildebrand, PhD⁷, Katherine R. Smith, PhD⁸, Melanie Bahlo, PhD^{8,9}, William J. Kimberling, PhD¹, Richard J. H. Smith, MD¹, Hela Azaiez, PhD¹ and Shelley D. Smith, PhD³

Purpose: The aim of this study was to determine the genetic cause of autosomal dominant nonsyndromic hearing loss segregating in a multigenerational family.

Methods: Clinical examination, genome-wide linkage analysis, and exome sequencing were carried out on the family.

Results: Affected individuals presented with early-onset progressive mild hearing impairment with a fairly flat, gently downsloping or U-shaped audiogram configuration. Detailed clinical examination excluded any additional symptoms. Linkage analysis detected an interval on chromosome 1p21 with a logarithm of the odds (LOD) score of 8.29: designated locus DFNA37. Exome sequencing identified a novel canonical acceptor splice-site variant c.652-2A>C in the *COL11A1* gene within the DFNA37 locus. Genotyping of all 48 family members confirmed segregation of this variant with the deafness phenotype in the extended family. The c.652-2A>C variant

is novel, highly conserved, and confirmed in vitro to alter RNA splicing.

Conclusion: We have identified *COL11A1* as the gene responsible for deafness at the DFNA37 locus. Previously, *COL11A1* was solely associated with Marshall and Stickler syndromes. This study expands its phenotypic spectrum to include nonsyndromic deafness. The implications of this discovery are valuable in the clinical diagnosis, prognosis, and treatment of patients with *COL11A1* pathogenic variants.

Genetics in Medicine (2019) 21:948–954; <https://doi.org/10.1038/s41436-018-0285-0>

Keywords: *COL11A1*; DFNA37; nonsyndromic hearing loss; splice-site variant; exome sequencing

INTRODUCTION

Hereditary hearing loss is a genetically heterogeneous disorder with over 150 genes implicated. Mirroring the genetic complexity is the breadth of phenotypic manifestations associated with pathogenic variants in these genes as more than 20% exhibit an extraordinary pleiotropy: they can give rise to either autosomal dominant nonsyndromic hearing loss (ADNSHL) or autosomal recessive nonsyndromic hearing loss (ARNSHL) (e.g., *TECTA* and *TMC1*) and they can cause syndromic hearing loss or nonsyndromic hearing loss (NSHL) (e.g., Usher type 1-causing genes, *WFS1*, *TBC1D24*, and *COL11A2*) (refs. ^{1–6}).

The collagen family is diverse and consists of more than 20 genetically distinct genes. Collagens are fibrous structural

proteins involved in the construction of skin, cartilage, bone, eye, and other tissues.^{7,8} All collagen molecules are comprised of three α -chain subunits tightly wrapped into a triple helix. The composition of each triple helix either contains one, two, or three different types of α -chains. For instance, the α -chains encoded by *COL11A1*, *COL11A2*, and *COL2A1* comprise a unique collagen fibril that is essential for proper skeletal and cartilage formation as well as ocular and auditory function.^{6,9,10}

The *COL11A1* gene, located on chromosome 1p21.1, consists of 67 exons spanning 232 Kb.¹¹ It encodes a peptide consisting of N- and C-terminal propeptides surrounding a collagen α -chain following the typical collagen Gly-X-Y repeat configuration. In the inner ear type XI collagens localize to the tectorial membrane, a gelatinous sheet-like structure

¹Molecular Otolaryngology and Renal Research Laboratories, Department of Otolaryngology, University of Iowa, Iowa City, IA, USA; ²Interdisciplinary Graduate Program in Molecular Medicine, Carver College of Medicine, University of Iowa, Iowa City, IA, USA; ³Developmental Neuroscience, Munroe Meyer Institute, University of Nebraska Medical Center, Omaha, NE, USA; ⁴Children's Mercy Hospital and University of Missouri-Kansas City School of Medicine, Kansas City, MO, USA; ⁵Department of Otorhinolaryngology, Radboud University Nijmegen Medical Centre, Nijmegen, Netherlands; ⁶DNA Microarray and Sequencing Core, University of Nebraska Medical Center, Omaha, NE, USA; ⁷Epilepsy Research Centre, Department of Medicine, University of Melbourne, Austin Health, Heidelberg, VIC, Australia; ⁸The Walter and Eliza Hall Institute of Medical Research, Parkville, VIC, Australia; ⁹Department of Medical Biology, The University of Melbourne, Parkville, VIC, Australia. Correspondence: Hela Azaiez (hela-azaiez@uiowa.edu) or Shelley D. Smith (shelley.smith@unmc.edu)

Co-first authors: Kevin T. Booth and James W. Askew

Submitted 26 April 2018; accepted: 16 August 2018

Published online: 24 September 2018

anchored to the apex of the interdental cells. The tectorial membrane lies on top of sensory hair cells and is comprised of four distinct types of collagen (types II, V, IX, and XI) and three primary noncollagenous glycoproteins (α -tectorin; Tecta, β -tectorin; Tectb, and Otogelin).¹²

Pathogenic variants in *COL11A1* have been linked to specific genetic disorders of the connective tissue, namely Marshall syndrome (MRSHS),¹³ Stickler syndrome type II (STL2) (refs. ^{14,15}), and fibrochondrogenesis (FBCG1) (ref. ¹⁶). Fibrochondrogenesis is an ultrarare disorder inherited in an autosomal recessive fashion. Affected individuals have severe skeletal defects characterized by pear-shaped vertebral bodies and broad long-bone metaphyses. Both Marshall and Stickler type 2 syndromes are rare autosomal dominant disorders. Clinically, there is much overlap between the two disorders because both include less severe vertebral and long-bone abnormalities; midface hypoplasia, which may include cleft palate; myopia with beaded vitreous; and mild to moderate hearing loss.

Until now, pathogenic variants in *COL11A1* have been exclusively linked to syndromic deafness. In this study, we present a novel splice-site altering variant in *COL11A1* that segregates in a large family with postlingual progressive ADNSHL and thus expands the phenotypic spectrum of pathogenic variants in *COL11A1*.

MATERIALS AND METHODS

Patients and clinical data

A four-generation family of European descent was ascertained as part of a genetic study of dominant progressive hearing loss at Boys Town National Research Hospital (BTNRH) between the years 1990 and 2000. After obtaining written informed consent from all participants with approval by the Institutional Review Board of BTNRH, pure tone audiograms and medical information were collected from participating family members. Clinical examination of the subjects excluded any additional syndromic findings. Blood samples from 48 family members were obtained and initial linkage studies were performed. The current studies were approved by the institutional review boards at the University of Nebraska Medical Center (UNMC) and the University of Iowa.

Audiograms and data analysis

Pure tone audiometry was performed according to current standards to determine air conduction thresholds at 0.25, 0.5, 1, 2, 4, 6, and 8 kHz. Bone conduction thresholds were determined at some frequencies in some patients to exclude conductive hearing impairment. After validating binaural symmetry, the binaural mean air conduction threshold (dB hearing level, HL) at each frequency was used for further analyses. Conduction loss was recorded for some individuals. For this reason the threshold data from individual IV:12 were excluded, as well as those obtained at age 6 years from individual III:17, and those obtained from the left ear in individual III:4.

Linear regression analyses of threshold on age were used to evaluate progression of hearing impairment at the separate

audio frequencies. These analyses comprised both individual longitudinal data derived from serial audiograms, and overall, cross-sectional last-visit data.¹⁷ Progression was called significant if the 95% confidence interval (95% CI) for slope did not include zero at two or more frequencies (out of 6 or 7, which is significant at $p < 0.05$ according to binomial distribution statistics, with $p = 0.025$ and $q = 0.975$ for positive correlations). The same applies to the threshold intercept. Progression was expressed in dB per year, and designated annual threshold deterioration (ATD). It was checked that the cross-sectional regression data conformed to the individual longitudinal regression data. Following that check, the regression data bearing on the last-visit thresholds were used to derive age-related typical audiograms (ARTA), which show the expected thresholds for a number of decade steps in age.¹⁷

Cross-sectional linear regression analyses were repeated for plots of threshold $-P50$ presby against age, where $P50$ presby is the median presbycusis predicted by the ISO 7029 norm¹⁸ according to each patient's gender and the age at which the audiogram was obtained.

Linkage analysis

Genome-wide linkage analysis was first conducted with microsatellite markers using an ABI Prism linkage mapping set and results were confirmed using the Affymetrix Xba chip (Affymetrix, Santa Clara, CA) with 50,000 single-nucleotide polymorphism (SNP) markers.¹⁹ Genotype calls were made with the BRLMM algorithm. Parametric multipoint linkage analysis was carried out using the Merlin program.

Exome sequencing and bioinformatic analysis pipeline

Four affected individuals (II.6, II.9, II.11, and III.9) underwent exome sequencing (ES) using the Agilent SureSelect Human All Exonv5 Kit (Agilent Technologies, Santa Clara, CA) as described^{2,20} (Fig. 1a). Prepared libraries were pooled and sequenced using an Illumina HiSeq 2000 (Illumina, San Diego, CA). We analyzed ES data using a custom bioinformatic pipeline. Reads were aligned to human reference genome (Human GRCh37/hg19) using Burrows–Wheeler Aligner (BWA). Variant calling was performed two ways: initially with the conservative Genome Analysis Toolkit (Broad Institute, Cambridge, MA), and later with the more inclusive SAMtools mpileup. Variants were annotated for conservation and deleteriousness using dbNSFP v2.0 (ref. ²¹), and for minor allele frequency (MAF) using the 1000 Genomes Project database, the Exome Aggregation Consortium database (ExAC) (<http://exac.broadinstitute.org/>), and the Genome Aggregation Database (gnomAD) (<http://gnomad.broadinstitute.org/>). Variant predicted effects on splicing were assessed using Human Splicing Finder (<http://www.umd.be/HSF3/>).

The following criteria were used for variant filtering: quality (depth $\geq 10\times$, Quality of Depth (QD) > 5 , quality > 30), MAF < 0.0001 , coding effect (nonsynonymous, indels, and splice-site variants), heterozygosity, and allele sharing amongst sequenced affected individuals.

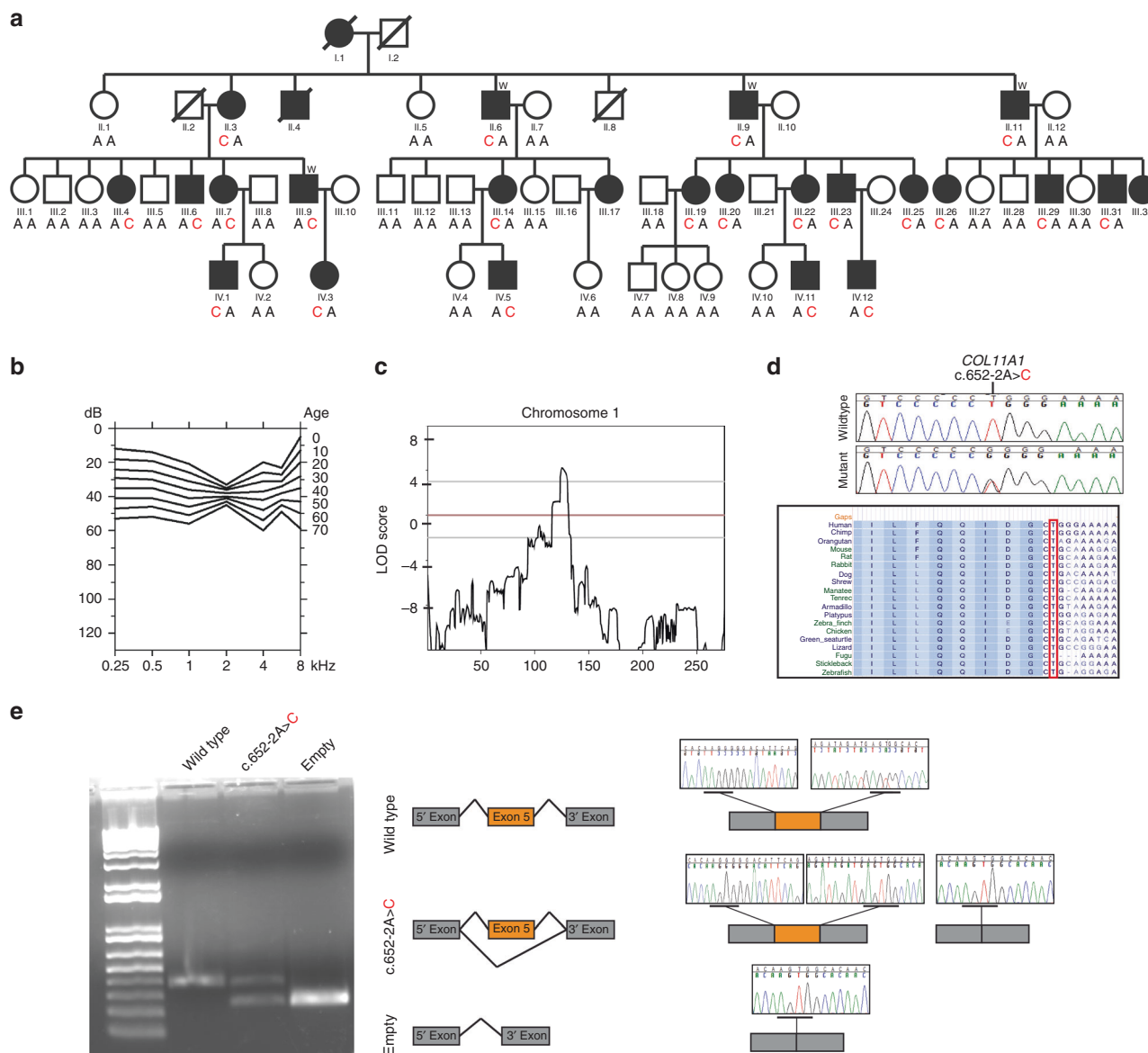


Fig. 1 Genetic Analysis of c.652A>C variant in COL11A1. **a** Family pedigree showing the segregation of the c.652-2A>C variant in COL11A1. Red and bold indicates the mutant allele. Circles and squares represent females and males, respectively. Filled symbols denote individuals with nonsyndromic hearing loss (NSHL) and nonfilled symbols show individuals with normal hearing. **b** Age-related typical audiograms (ARTA). Binaural mean air conduction thresholds (dB HL) are presented for the ages 10–60 years. **c** Parametric linkage analysis plot of chromosome 1. **d** Representative chromatograms from wild-type and mutant sequences. **e** Gel electrophoresis of wild-type COL11A1 exon 5, c.652-2A>C pathogenic variant, and the empty pET01 vector. The inclusion of exon 5 results in a 372-bp product and its exclusion results in a 234-bp band. Sequence chromatograms show read through at each exon junction. Results shown from COS7 experiments. LOD logarithm of the odds.

Segregation analysis

Sanger sequencing was completed in available family members to confirm segregation of all candidate variants (Table S1); c.652-2A>C in COL11A1 gene (MIM 120280; NM_080629.2), c.70C>T:p.R24W in ARHGEF16 (NM_014448.3), and c.847G>A:p.E283K in TRABD (NM_001320484.1).

Minigene splicing assay

In vitro minigene assays were carried out as described.²² Briefly, wild-type exon 5 and ~120 base pairs of each flanking intron of COL11A1 were polymerase chain reaction (PCR) amplified and ligated into the pET01 vector

(MoBiTec, Goettingen, Germany). The c.652-2A>C variant was introduced to the wild-type vector using the QuikChange Lightning Site-Directed Mutagenesis kit (Agilent, Santa Clara, CA, USA) according to the manufacturer’s protocol. Wild-type or mutant vectors were transfected into COS7 and HEK293 cells in triplicate. Total RNA was harvested 48 h posttransfection and complementary DNA (cDNA) was transcribed according to the manufacture protocol. PCR using primers specific to the 5’ and 3’ native exons of the pET01 vector was performed and products were visualized on an agarose gel. Gel products were extracted and Sanger sequenced.

RESULTS

Clinical presentation

The family ascertained in this study is a four-generation kindred of European descent segregating hearing loss as an autosomal dominant trait (Fig. 1a). Pure tone audiometric evaluation of affected members showed bilateral, postlingual, progressive sensorineural hearing loss (Fig. 1b). The hearing loss was mild to moderate and progressed slowly. The finding of a significant threshold intercept at age 0 years (Figure S2) at all frequencies except 8 kHz (Figure S2) suggests the presence of a substantial congenital component (of 12 to 23 dB) to the SNHL. As shown by the ARTA depicted in Fig. 1b, the mean audiogram configuration developed from U-shaped (mid-frequency type) to flat with advancing age up to ~40 years. At more advanced ages it remained flat or became very gently downsloping (Fig. 1b, S1).

To evaluate progression of hearing impairment at each frequency, we performed linear regression analyses of threshold on age. The resulting ATD (progression) was significant at 5 of 7 frequencies (significant): 0.25–1 kHz, 4 and 8 kHz. It varied between 0.2 and 0.8 dB per year (Figure S2). This variation is also reflected by the ARTA (Fig. 1b). One-way analysis of variance (ANOVA) followed by Tukey's multiple comparison test showed that the ATD at 2 kHz was significantly smaller than the ATD at all other frequencies, whereas the ATD at 8 kHz was significantly greater than the ATD at all other frequencies, except for 0.25 and 4 kHz. The ATD for the thresholds corrected for median presbycusis was significantly positive at 0.25–1 kHz (Figure S3). This suggests SNHL progression beyond presbycusis at these lower frequencies. The ATD at the higher frequencies did not differ significantly from zero, even though the values at 6–8 kHz were negative. This implies that progression at 2–8 kHz conformed with expected presbycusis. Clinical examination of affected members excluded any additional syndromic features usually associated with Marshall syndrome and Stickler syndrome as the craniofacial features of affected family members were normal. X-ray images of the long bones of the proband (III-19) were also normal. There was no history of ocular abnormalities or cleft palate in the family.

Linkage analysis

The initial linkage analysis identified a single region on chromosome 1p21 spanning ~12 Mb between markers D1S497 and D1S2651 with a maximum LOD score of 8.29 for marker D1S195 (ref. ¹⁹). This linked interval was designated DFNA37. A second genome-wide linkage using the Affymetrix Xba chip narrowed down the linked interval to a ~8.4 Mb region between markers rs724480 and rs6667402 (Fig. 1c, S4).

Exome sequencing and variant assessment

Capitalizing on the advances made in sequencing technologies, we used ES to screen four affected individuals (II.6, II.9, II.11, and III.9). An average depth of coverage of 114 reads

was obtained with 92% of targeted regions covered at $\geq 30\times$ (Table S2). After filtering for quality, MAF, coding effect (nonsynonymous, indels, and splice-site variants), heterozygosity, and allele sharing amongst sequenced affected individuals in the DFNA37 locus, only one variant in *COL11A1* was identified. The variant NM_080629.2; c.652-2A>C (chr1:103496802T>G) affects the canonical splice site in intron 4 resulting in the alteration of the acceptor site (AG to CG) confirmed by analysis with Human Splicing Finder 3.0 and NNSPLICE 0.9. Sanger sequencing performed on all family members showed the segregation of c.652-2A>C variant at a heterozygous state with the deafness phenotype in the extended family (Fig. 1a, d). This splice-site variant is predicted to cause skipping of exon 5 and a production of a protein lacking residues 218–260 in the N-propeptide domain.

Splicing analysis

To characterize the impact of the c.652-2A>C variant on RNA splicing, we cloned the wild-type and mutant sequences of *COL11A1* exon 5 and flanking introns into the pET01 exon trap vector and transfected them into two different cell lines. Visualization of the splicing products revealed that cells transfected with the wild-type vector yielded the expected 372-bp band containing exon 5 (Fig. 1e). In contrast, cells transfected with the mutant vector yielded two bands; one at 372 bp corresponding to the wild-type allele and the second at 234 bp lacking exon 5. These results were identical across both cell lines. Sequencing all bands confirmed break points and splicing events.

DISCUSSION

Coupling linkage analysis and ES, we identified a novel splice-site altering variant (c.652-2A>C) in the *COL11A1* gene segregating in a large European-American pedigree with postlingual progressive ADNSHL. The DFNA37 locus was mapped almost two decades ago but screening methodologies at the time failed to detect causative alterations in *COL11A1* (ref. ¹⁹). Since mapping of DFNA37, knowledge of genomic sequences has improved substantially. In addition, development of next-generation sequencing has proven useful in elucidating the genetic causes of Mendelian disorders and notably, hereditary deafness.²³ We capitalized on these new technologies to reevaluate the DFNA37 locus for pathogenic variants and identified the genetic cause underlying hearing loss in this family.

The heterozygous c.652-2A>C variant in *COL11A1* we identified segregating with the NSHL in this family is novel (absent from all population databases), highly conserved, and predicted to abolish the acceptor splice site of exon 5 by in silico analysis. We confirmed aberrant splicing of exon 5 due to c.652-2A>C in vitro using a minigene splicing assay (Fig. 1e). Interestingly, the c.652-2A>C variant seems to affect splicing efficiency rather than completely abolishing it. These findings suggest the c.652-2A>C variant creates a leaky acceptor splice site that allows for some expression of a

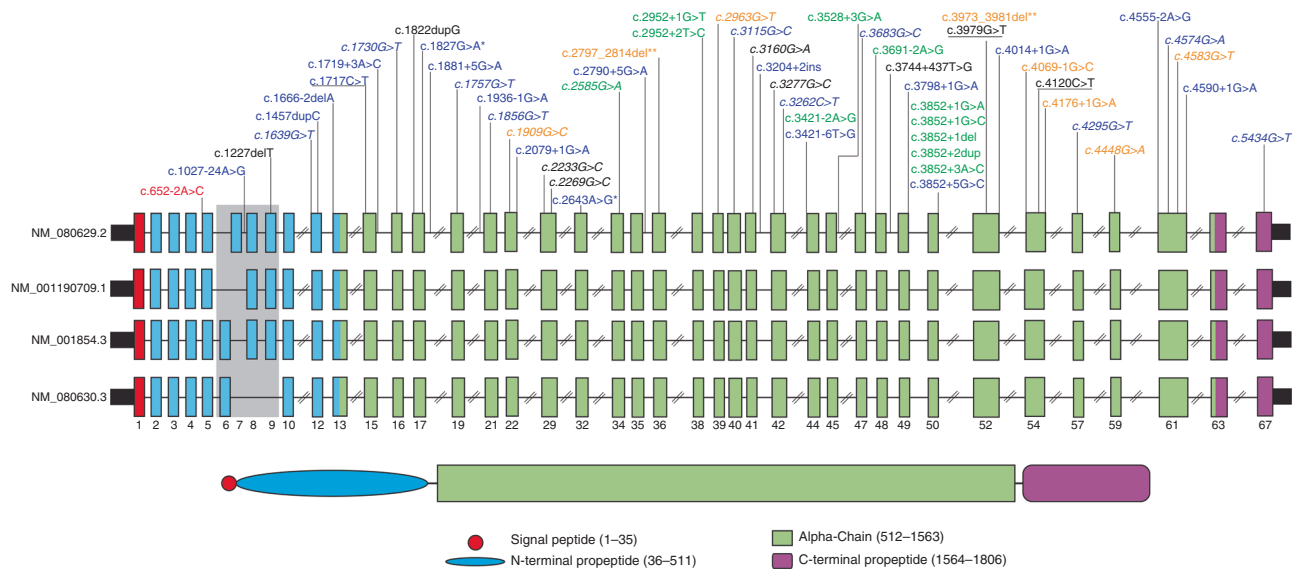


Fig. 2 *COL11A1* gene and protein schematic denoting pathogenic variants and their associated phenotypes. All variants were collected from the Deafness Variation Database (DVD; <http://deafnessvariationdatabase.org/>). The gray box shows the alternatively spliced exons. Text colored blue, black, green, and orange indicates the phenotypes associated with pathogenic variants in *COL11A1*: STL2, FBCG1, MRSFS, and STL2/MRSFS, respectively. Missense variants are in italics and nonsense variants are underlined. An asterisk (*) denotes a synonymous change, while a double asterisk (**) represents in-frame indels. The position of the c.652-2A>C pathogenic variant is shown in red and bold. Nucleotide numbering: the A of the ATG translation initiation site is noted as +1 using transcript NM_001854.3.

normal spliced transcript. This might explain the audiometric variability seen among some affected individuals, such as the manifestation of conductive hearing loss seen in III.4 and IV.12 or the diversity of audiometric configurations between individuals which could be flat, gently downsloping or U-shaped (Figure S1). Exon 5 is the last exon before the start of the variable region (exons 6, 7, 8, and 9) thus the c.652-2A>C variant would affect splicing in all five transcripts of *COL11A1* (Fig. 2). Aberrant splicing leading to exon 5 skipping would result in an in-frame deletion and *COL11A1* peptides lacking residues 218–260 in the N-terminal propeptide (Fig. 2). It is also possible that other splicing events occur that could not be detected with the current minigene design. Analysis of RNA from individuals harboring the c.652-2A>C variant would better define the splicing defects resulting from this variant.

The exact function of N-terminal propeptide remains unclear. However, it is known to have a role in regulating the shape and size of the collagen fiber.²⁴ Lacking the amino acids encoded by exon 5 could result in a collagen fibril with a different diameter or shape, due to loss of key N-terminal propeptide regulatory sequences, such as the heparan sulfate binding motif that is located between residues 147–152 (refs. ^{25,26}). Alternatively, it may result in protein misfolding as this domain also houses two structurally important cysteine residues at amino acids 236 and 243, which are important to disulfide bond formation with other cysteines at positions 182 and 61. In the inner ear, *COL11A1* is expressed in the tectorial membrane. Within the tectorial membrane, collagens form two networks of fibers: one unbranched, parallel, and coordinated mainly by noncollagenous proteoglycans. The

second, a striated sheet structure, is orientated via the cross bridges and glycoproteins. Loss of this organization at either the collagenous or noncollagenous level causes hearing loss in mice and humans.^{5,27} Because the N-propeptide domain plays a role in the establishment of molecular interactions with several extracellular matrix molecules and cellular proteins such as heparan sulfate proteoglycans and calcium, its alteration might impair its binding affinity for these molecules.^{25,28} This could hamper interactions between cells and the surrounding extracellular matrix, as well as interactions between the diverse constituents of the extracellular matrix.

Regardless of the variant effect, it is clear the residues encoded by exon 5 are essential for proper auditory function. The absence of any other phenotypic manifestations in the described family is remarkable, given all previously reported autosomal dominant pathogenic variants (>50) have been only associated with either STL2 or MRSFS (Fig. 2). However, the splice-site variant identified in this study is the first pathogenic alteration reported in the nonvariable region of the N-propeptide domain. The majority of pathogenic variants in *COL11A1* are splice-altering located in the triple-helical domain and thought to exert their effect via a dominant-negative mechanism. This is further supported by studies in mouse showing that mice homozygous for a spontaneous frameshift pathogenic variant in *Coll1a1* have severe chondrodysplasia and die at birth. Heterozygous mice escape lethality, develop osteoarthritis, and have normal auditory responses up to 10 months postnatally.²⁹ The lack of an auditory phenotype in the heterozygous mouse suggests haploinsufficiency is not the pathogenic mechanism

underlying *COL11A1*-related auditory defects in humans. Pleiotropy associated with deafness-causing genes, where pathogenic variants in the same gene could cause either syndromic or nonsyndromic hearing loss, has been demonstrated for several other genes such as the genes involved in Usher syndrome (*PCDH15*; *DFNB23/USH1F*, *USH1C*; *DFNB18A/USH1C*, *WHRN*; *DFNB31/USH2D*, *MYO7A*; *DFNB2/DFNA11/USH1B*, *CDH23*; *DFNB12/USH1D*), *WFS1* (*DFNA6/14/38/Wolfram syndrome*), *TBC1D24* (*DFNA65/DFNB86/DOORS syndrome*), and *COL11A2* (*DFNB53/DFNA13/STL3*) (refs.^{1–3,5}).

The present *DFNA37* patients with a *COL11A1* pathogenic variant showed fairly similar audiograms to those reported for *DFNA* traits with a midfrequency type of hearing impairment: *DFNA8/12 (TECTA)* and *DFNA13 (COL11A2)* (refs.^{30,31}). The *DFNB* phenotypes that are allelic to these traits also show midfrequency-like types of audiograms, but usually at substantially higher thresholds: *DFNB21 (TECTA)* and *DFNB53 (COL11A2)* (refs.^{32,33}). Patients with collagenopathies that include hearing impairment due to deleterious variants in *COL11A1* (*STL2* and *Marshall syndrome*) and *COL11A2* (*STL3*) also show remarkably similar types of audiograms.^{34–36} The results of psychophysical tests at suprathreshold levels in *DFNA8/12*, *DFNA13*, and *STL3 (COL11A2)* patients revealed that the type of hearing impairment is compatible with intracochlear conduction loss.^{36–38} This is in line with the notion that disease-causing variants in *COL11A2* affect tectorial membrane function.^{31,39} Recent work on cochlear (micro)mechanics involving animal models with genetic modifications has provided compelling evidence about the relevant mechanical changes that can be involved.^{5,12,39}

In summary, here we report the clinical and genetic characteristics associated with deafness at the *DFNA37* locus and we expand the spectrum of *COL11A1*-associated phenotypes to include *ADNSHL*. This study illustrates another example of the pleiotropy exhibited by other deafness-causing genes and highlights the complexity associated with providing the correct genetic diagnosis.

ELECTRONIC SUPPLEMENTARY MATERIAL

The online version of this article (<https://doi.org/10.1038/s41436-018-0285-0>) contains supplementary material, which is available to authorized users.

ACKNOWLEDGEMENTS

We would like to thank all family members reported here for their collaboration in this study. Z.T. also acknowledges the helpful advice of Stefan Stamm (University of Kentucky) in the interpretation of splice-site variants. Funding for this study was provided by the National Institute on Deafness and Other Communication Disorders (NIDCD) R01s DC02942 to S.D.S.; R01s DC003544, DC002842, and DC012049 to R.J.H.S., and the Omaha Community Foundation (S.D.S.). The UNMC DNA Sequencing Core facility is also supported by P30 GM110768: Core B Sequencing (J.D.E., S.D.S.).

DISCLOSURE

The authors declare no conflicts of interest.

REFERENCES

- Bork JM, Peters LM, Riazuddin S, Bernstein SL, Ahmed ZM, Ness SL, et al. Usher syndrome 1D and nonsyndromic autosomal recessive deafness *DFNB12* are caused by allelic mutations of the novel cadherin-like gene *CDH23*. *Am J Hum Genet*. 2001;68:26–37.
- Azaiez H, Booth KT, Bu F, Huygen P, Shibata SB, Shearer AE, et al. *TBC1D24* mutation causes autosomal-dominant nonsyndromic hearing loss. *Hum Mutat*. 2014;35:819–823.
- Cryns K, Sivakumaran TA, Van den Ouweland JMW, Pennings RJE, Cremers CWRJ, et al. Mutational spectrum of the *WFS1* gene in Wolfram syndrome, nonsyndromic hearing impairment, diabetes mellitus, and psychiatric disease. *Hum Mutat*. 2003;22:275–287.
- Rigoli L, Lombardo F, Di Bella C. Wolfram syndrome and *WFS1* gene. *Clin Genet*. 2011;79:103–117.
- Richardson GP, de Monvel JB, Petit C. How the genetics of deafness illuminates auditory physiology. *Annu Rev Physiol*. 2011;73:311–334.
- Acke FRE, Dhooze IJM, Malfait F, De Leenheer EMR. Hearing impairment in Stickler syndrome: a systematic review. *Orphanet J Rare Dis*. 2012;7:84.
- Ricard-Blum S. The collagen family. *Cold Spring Harb Perspect Biol*. 2011;3:1–19.
- Spranger J. The type XI collagenopathies. *Pediatr Radiol*. 1998;28:745–750.
- Myllyharju J, Kivirikko KI. Collagens and collagen-related diseases. *Ann Med*. 2001;33:7–21.
- Keene DR, Oxford JT, Morris NP. Ultrastructural localization of collagen types II, IX, and XI in the growth plate of human rib and fetal bovine epiphyseal cartilage: type XI collagen is restricted to thin fibrils. *J Histochem Cytochem*. 1995;43:967–979.
- Henry I, Bernheim a, Bernard M, van der Rest M, Kimura T, Jeanpierre C, et al. Mapping of a human fibrillar collagen gene, pro alpha 1 (XI) (*COL11A1*), to the p21 region of chromosome 1. *Genomics*. 1988;3:87–90.
- Richardson GP, Lukashkin AN, Russell IJ. The tectorial membrane: one slice of a complex cochlear sandwich. *Curr Opin Otolaryngol Head Neck Surg*. 2008;16:458–464.
- Annunen S, Kórkö J, Czarny M, Warman ML, Brunner HG, Käriäinen H, et al. Splicing mutations of 54-bp exons in the *COL11A1* gene cause Marshall syndrome, but other mutations cause overlapping Marshall/Stickler phenotypes. *Am J Hum Genet*. 1999;65:974–983.
- Majava M, Hoornaert KP, Bartholdi D, Bouma MC, Bouman K, Carrera M, et al. A report on 10 new patients with heterozygous mutations in the *COL11A1* gene and a review of genotype–phenotype correlations in type XI collagenopathies. *Am J Med Genet A*. 2007;143A:258–264.
- Rose PS, Levy HP, Liberfarb RM, Davis J, Szymko-Bennett Y, Rubin BI, et al. Stickler syndrome: clinical characteristics and diagnostic criteria. *Am J Med Genet A*. 2005;138A:199–207.
- Tompson SW, Bacino CA, Safina NP, Bober MB, Proud VK, Funari T, et al. Fibrochondrogenesis results from mutations in the *COL11A1* type XI collagen gene. *Am J Hum Genet*. 2010;87:708–712.
- Huygen PLM, Pennings RJE, Cremers CWRJ. Characterizing and distinguishing progressive phenotypes in nonsyndromic autosomal dominant hearing impairment. *Audiol Med*. 2003;1:37–46.
- Stenklev NC, Laukli E. Presbycusis—hearing thresholds and the ISO 7029. *Int J Audiol*. 2004;43:295–306.
- Talebizadeh Z, Kenyon J, Askew J, and Smith S (2000). A new locus for dominant progressive hearing loss *DFNA37* mapped to chromosome 1p21. Presented at the American Society of Human Genetics, 10/05/2000, Philadelphia, PA. Printed in the American Journal of Human Genetics 67(Suppl.2):314.
- Azaiez H, Decker AR, Booth KT, Simpson AC, Shearer AE, Huygen PLM, et al. *HOMER2*, a stereociliary scaffolding protein, is essential for normal hearing in humans and mice. *PLoS Genet*. 2015;11:e1005137.
- Liu X, Jian X, Boerwinkle E. dbNSFPv2.0: a database of human non-synonymous SNVs and their functional predictions and annotations. *Hum Mutat*. 2013;34:2393–2402.
- Booth KT, Azaiez H, Kahrizi K, Wang D, Zhang Y, Frees K, et al. Exonic mutations and exon skipping: lessons learned from *DFNA5*. *Hum Mutat*. 2018;39:433–440.

23. Vona B, Nanda I, Hofrichter MAH, Shehata-Dieler W, Haaf T. Nonsyndromic hearing loss gene identification: a brief history and glimpse into the future. *Mol Cell Probes*. 2015;29:260–270.
24. Hulmes DJS. Building collagen molecules, fibrils, and suprafibrillar structures. *J Struct Biol*. 2002;137:2–10.
25. Warner LR, Brown RJ, Yingst SMC, Oxford JT. Isoform-specific heparan sulfate binding within the amino-terminal noncollagenous domain of collagen alpha1(XI). *J Biol Chem*. 2006;281:39507–39516.
26. McDougal OM, Warner LR, Mallory C, Oxford JT. Predicted structure and binding motifs of collagen A1(XI). *GSTF Int J Bioinforma Biotechnol*. 2011;1:43–48.
27. Petit C, Richardson GP. Linking genes underlying deafness to hair-bundle development and function. *Nat Neurosci*. 2009;12:703–710.
28. Kearney HM, Thorland EC, Brown KK, Quintero-Rivera F, South ST. American College of Medical Genetics standards and guidelines for interpretation and reporting of postnatal constitutional copy number variants. *Genet Med*. 2011;13:680–685.
29. Rodriguez RR, Seegmiller RE, Stark MR, Bridgewater LC. A type XI collagen mutation leads to increased degradation of type II collagen in articular cartilage. *Osteoarthritis Cartilage*. 2004;12:314–320.
30. Hildebrand MS, Morin M, Meyer NC, Mayo F, Modamio-Hoybjor S, Mencia A, et al. DFNA8/12 caused by TECTA mutations is the most identified subtype of nonsyndromic autosomal dominant hearing loss. *Hum Mutat*. 2011;32:825–834.
31. McGuirt WT, Prasad SD, Griffith AJ, Kunst HPM, Green GE, Shpargel KB, et al. Mutations in COL11A2 cause non-syndromic hearing loss (DFNA13). *Nat Genet*. 1999;23:413–419.
32. Meyer NC, Alasti F, Nishimura CJ, Imanirad P, Kahrizi K, Riazalhosseini Y, et al. Identification of three novel TECTA mutations in Iranian families with autosomal recessive nonsyndromic hearing impairment at the DFNB21 locus. *Am J Med Genet A*. 2007;143:1623–1629.
33. Chen W. Mutation of COL11A2 causes autosomal recessive non-syndromic hearing loss at the DFNB53 locus. *J Med Genet*. 2005;42:e61–e61.
34. Acke FR, Swinnen FK, Malfait F, Dhooze IJ, De Leenheer EMR. Auditory phenotype in Stickler syndrome: results of audiometric analysis in 20 patients. *Eur Arch Oto-Rhino-Laryngol*. 2016;273:3025–3034.
35. Griffith AJ, Gebarski SS, Shepard NT, Kileny PR. Audiovestibular phenotype associated with a COL11A1 mutation in Marshall syndrome. *Arch Otolaryngol Head Neck Surg*. 2000;126:891–894.
36. van Beelen E, Leijendeckers JM, Huygen PLM, Admiraal RJC, Hoefsloot LH, Lichtenbelt KD, et al. Audiometric characteristics of two Dutch families with non-ocular Stickler syndrome (COL11A2). *Hear Res*. 2012;291:15–23.
37. Plantinga RF, Cremers CWRJ, Huygen PLM, Kunst HPM, Bosman AJ. Audiological evaluation of affected members from a Dutch DFNA8/12 (TECTA) family. *J Assoc Res Otolaryngol*. 2007;8:1–7.
38. De Leenheer EMR, Busman AJ, Huygen PLM, Kunst HPM, Cremers CWRJ. Audiological characteristics of some affected members of a Dutch DFNA13/COL11A2 family. *Ann Otol Rhinol Laryngol*. 2004;113:922–929.
39. Masaki K, Gu JW, Ghaffari R, Chan G, Smith RJH, Freeman DM, et al. Col11a2 deletion reveals the molecular basis for tectorial membrane mechanical anisotropy. *Biophys J*. 2009;96:4717–4724.



Open Access This article is licensed under a Creative Commons Attribution 4.0 International License, which permits use, sharing, adaptation, distribution and reproduction in any medium or format, as long as you give appropriate credit to the original author(s) and the source, provide a link to the Creative Commons license, and indicate if changes were made. The images or other third party material in this article are included in the article's Creative Commons license, unless indicated otherwise in a credit line to the material. If material is not included in the article's Creative Commons license and your intended use is not permitted by statutory regulation or exceeds the permitted use, you will need to obtain permission directly from the copyright holder. To view a copy of this license, visit <http://creativecommons.org/licenses/by/4.0/>.

© The Author(s) 2018